© Universiti Tun Hussein Onn Malaysia Publisher's Office

JAMEA

http://penerbit.uthm.edu.my/ojs/index.php/jamea

e-ISSN: 2716-6201

Journal of Advanced Mechanical Engineering Applications

Research Advances on 2D Mxenes for Photovoltaic Applications

Opeyemi Akanbi[1], Gbemi Abass[2]*, Akinsanmi Ige[1], Daniel Nyatse[3], Hakeem Oyeshola[1], Haruna Abba[4], Olusegun Felix[5], Kehinde Oni[6], Alabi Ayotunde[5], Joshua Ajao[7], Hammed Akinade[8], Abiodun Oladejo[8], Olusola Akinrinola[1]

[1]Department of Pure and Applied Physics,
Ladoke Akintola University of Technology, Ogbomosho, 210214, NIGERIA

[2]Department of Materials Science and Engineering,
Hohai University, Nanjing, 210098, CHINA

[3]Department of Chemical Engineering,
Ahmadu Bello University, Zaria, 810106, NIGERIA

[4]Department of Mechanical Engineering,
Jigawa State Polytechnic, Dutse, 720102, NIGERIA

[5]Department of Chemical Engineering,
Obafemi Awolowo University, Ile-Ife, 220282, NIGERIA

[6]Department of Mechanical Engineering,
Ekiti State University, Ado Ekiti, 362103, NIGERIA

[7]Department of Chemical Engineering,
Ladoke Akintola University of Technology, Ogbomoso, Oyo State, 210214, NIGERIA

[8]Department of Electronics and Electrical Engineering,
Ladoke Akintola University of Technology, Ogbomoso, 210214, NIGERIA

*Corresponding Author

DOI: https://doi.org/10.30880/jamea.2023.04.01.006
Received 2 January 2023; Accepted 16 March 2023; Available online 28 June 2023

Abstract: MXene, a two-dimensional nanomaterial, has an impressive range of properties that make it a perfect choice for a variety of applications, including energy systems, high-tech sensors, optics, medical devices, and electromagnetic interference shielding. Its high carrier mobility, metallic electrical conductivity, superior transparency, excellent mechanical characteristics, and tunable work function have drawn much attention. This review examines the utilization of MXene in solar technology, highlighting its potential as an electrode, charge carrier, and additive in quantum dot-sensitized, perovskite, silicon wafer-based, and organic solar cells. Additionally, a summary table is provided that briefly outlines the different methods of synthesizing MXene and their respective etching chemicals and precursors. This review's latter part looks at the challenges associated with MXene and offers potential solutions and prospects.

Keywords: Two-dimensional (2D) material, MXene, solar energy, nanomaterials, titanium carbide

*Corresponding author: abass.gbemi@gmail.com

1. Introduction

After uncovering the special physical properties of single-layer graphene, two-dimensional (2D) materials became an incredibly active and interesting field of research [1], which then drew attention to other 2D materials besides graphene. This also accelerated the analysis of different materials with easily accessible layered precursors such as dichalcogenides and layered oxides, as well as hexagonal boron nitride (h-BN) which is graphite-like [2]. It was then proven that there were no weakly bound layered precursors for two-dimensional (2D) Germanium [3], Silicon [4], Tin [5], and other materials, which was an indication that the range of 2D materials was likely to expand and include various substances with different structures and chemistries. One of these 2D materials, MXene, was first created (see Fig. 1) in 2011 [6-8] and has since become one of the most popular 2D materials. $M_{n+1}X_nT_x$ (n = 1- 3) is the universal formula for MXenes, and they are two-dimensional transition nitrides, carbonitrides, and metal carbides. The metal component of the compound can range from molybdenum, scandium, zirconium, hydrogen fluoride, titanium, vanadium, niobium, chromium, and tantalum, which are early transition metals. X can be either nitrogen, carbon, or both, and T_x refers to the surface terminations (oxygen, fluorine, or hydroxyl) (see Fig. 7 and 8) [9-11]. Currently, there are over thirty different types of MXenes that have been synthesized (as summarized in Table 1), each with its own unique stoichiometric composition. In theory, there is an infinite amount of MXene solid solutions that could be created, and many of them are still being studied [12-14]. MXene has various physical and chemical properties, such as low optical attenuation [15], good electrical conductivity [16-19], tunable bandgap [20], and remarkable photoelectronic properties due to its programmable surface terminations [13, 21], and diverse fundamental compositions. There is a wide range of applications for MXenes, including sensors [12, 22], conversion and storage of energy [23-25], electromagnetic interference shielding [26], absorption [27], electrocatalysis [28-30], and photocatalysis [18, 31, 32].

MXenes can be used in solar cells in a variety of ways, including as an additive, an electrode, and a hole/electron transport layer. When used as an additive, MXenes have been shown to increase the crystal size and accelerate the electron transfer rate, thus improving power conversion efficiency. Additionally, the work function of the MXenes can be adjusted without impacting the other intrinsic properties of the perovskite nanoflakes. MXenes are known for their excellent flexibility, variable work function, high conductivity, and high transparency, making them ideal for use as electrodes in solar cells. They can also be used in various solar cell designs, such as flexible hybrid, common, and back electrodes. Compared to other electrodes, such as indium tin oxide (ITO) and carbon, MXene-based electrodes can lead to higher power conversion efficiency, hole injection rate, reduced series resistance, and open-circuit voltage. Furthermore, MXenes can be used to facilitate charge transfer as a transparent conducting electrode. In MXene silicon-based heterojunction solar cells, MXenes can be used to help separate electron-hole pairs, as well as to create a built-in potential at the solar cell junction. Additionally, the charge separation efficiency between the silicon and MXene can be increased due to the adjustable work function of MXenes.

Solar energy can help reduce the emission of greenhouse gases, which is essential for the preservation of ecosystems, animals, and people. It can also improve the quality of air. The first-generation crystalline silicon solar cell is the most common and efficient type of solar cell, although it is costly to produce and maintain. Even though the second-generation thin-film-based solar cells are cheaper than previous versions, they are not as effective. The newest solar cells, such as organic, perovskites, and dye-synthesized solar cell systems, are beginning to provide groundbreaking, cost-effective solar materials made from nano-sized components. A few-atom-thick layer of carbonitrides, nitrides, and transition metal carbides known as MXene is a set of recently discovered two-dimensional materials that exhibits good thermal, electrical, and ion transport characteristics [33]. This review looks at how MXene can be used as additives, electrodes, and charges to enhance the research and commercial use of MXene-based materials for photovoltaic applications. It also covers MXene synthesis (which is summarized in Table 1) and how this can affect solar energy harvest. Additionally, the future perspective (see Fig. 1) and various methods of increasing the performance of MXene are investigated.

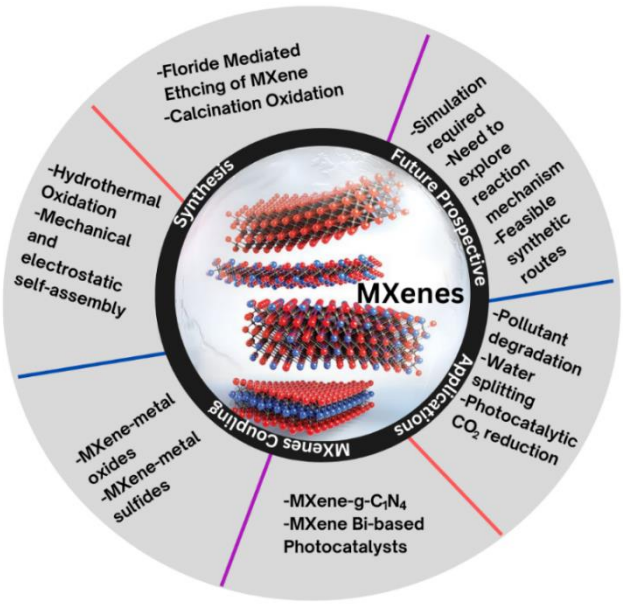

Fig. 1 - Outline of nanocomposites based on MXenes for solar energy harvesting [34]

1.1 Methods of Synthesis

Two distinct approaches can be used to produce two-dimensional layered nanomaterial: (i) the top-down technique and (ii) the bottom-up method. Both methods have been utilized in creating MXene with single or many layers.

Table 1 - Recent advancements in the stable MXene production process

MXenes(Mn+1XnTx)	Etching chemicals	Precursors	Therapy to increase stability	Duration of Stability (seconds)	Year and References
SA- $Ti_3C_2T_x$	LiF–HCl	Titanium aluminum carbide	binding molecules with $C_6H_7O_6Na$	6,912,000	2020 [35]
$Ti_3C_2T_x$	LiF–HCl	Titanium aluminum carbide	193.15K freeze storage	23,587,200	2019 [36]
$Ti_3C_2T_x$	LiF–HCl	Titanium aluminum carbide	253.15K freeze storage	56,160,000	2020 [37]
V_2CT_x	Hydrogen fluoride	Vanadium aluminum carbide	The use of polyanionic salts (polyP) for edge capping	2,592,000	2019 [38]
r- $Ti_3C_2T_x$	Hydrogen fluoride	Titanium aluminum carbide	L- $C_6H_8O_6$	2,419,200	2020 [39]
$Ti_3C_2T_x$	LiF–HCl	Titanium aluminum carbide	The use of polyanionic salts (polyP) for edge capping	2,592,000 (in an exposed bottle)	2019 [38]
Titanium-Carbide (Ti_3C_2)	Mud Acid	Al-Titanium aluminum carbide	Ti_3AlC_2 was synthesized with a modified process to create Al - Ti_3AlC_2, which is more stoichiometric.	25,920,000	2020 [40]

2. MXene (Ti3C2Tx) for Photovoltaic Application

2.1 Incorporating Mxene into Perovskite Materials as an Additive

In 2018, research on MXenes for solar cell application was jumpstarted by Guo et al.'s exploration of the addition of titanium carbide (the first MXene to be reported for solar cell application) to the methylammonium lead iodide ($MAPbI_3$) -based perovskite absorber [41]. This research showed that the addition of MXene ($Ti_3C_2T_x$) could delay the nucleation of $MAPbI_3$ and lead to an increase in crystal size (Fig. 2(a)). Additionally, the $Ti_3C_2T_x$ additive, which acts as a "carrier bridge," was particularly effective in increasing electron transmission across the grain boundary [42–45]. The electrochemical impedance spectrum of the device with $Ti_3C_2T_x$ added also revealed lower charge-transfer resistance (Fig. 2(b)). By the end of the process, the average power conversion efficiency (PCE) rose from 15.18 percent to 16.8 % when tested in AM 1.5G illumination.

Agresti *et al*. explored the potential to modify the work function of $MAPbI_3$ films in a study they published in 2019 [20, 46]. By introducing titanium carbide ($Ti_3C_2T_x$), it was found that the energy level of the associated solar cells could be optimized without affecting the film morphology or bandgap. When $Ti_3C_2T_x$ was added to the $MAPbI_3$ solar cells, their power conversion efficiency (PCE) increased by 26.5%, compared to the control cell without the addition of $Ti_3C_2T_x$. This was achieved by including $Ti_3C_2T_x$ in the electron transport layer. Fig. 2(c), as reported by Zhang et al., illustrates how freshly prepared titanium carbide nanosheets ($Ti_3C_2T_x$) were used to decorate the nanocrystals of $MAPbBr_3$, forming an MXene heterostructure [36, 47]. As can be observed in Figure 2d, the efficiency of the related solar cell was improved due to the alignment of energy levels. This was made possible by the injection of electrons into $Ti_3C_2T_x$, which was enabled by the nanocrystals of $MAPbBr_3$.

Chen et al. implemented ultra-thin $Ti_3C_2T_x$ quantum dots (TQDs) at the perovskite/TiO_2 electron transport layer interface with the CsFAMA perovskite absorber, as displayed in Fig. 2(e) [48]. This allowed for improved electron extraction at the interface, and an increase in the crystallinity of the perovskite film, and the alignment of corresponding energy levels (Fig. 2(f)). This led to an enhanced solar cell with superior light stability and ambient stability for the long-term, with a hysteresis-free power conversion efficiency of 20.72%, when compared to the reference device with an efficiency of 18.31%. In addition, the increased hole extraction at the interface of the perovskite/Spiro-OMeTAD hole transport layer and the help of perovskite crystallinity when $Cu_{1.8}S$ is added to the hole transport layer, outlined in Fig. 2(f), also contributed to the improved performance and durability.

Recently, Hou et al. examined the effects on the electrical conductivity of introducing the $Ti_3C_2T_x$ MXene nanosheet to the conductive polymer poly(3,4 ethylene dioxythiophene): poly(styrene sulfonate) (PEDOT: PSS), which is usually used as the hole transport layer in organic solar cells [49]. As seen in Fig. 3(a), the MXene nanosheet produces additional charge transfer channels between PEDOT nanocrystals, as indicated by the conductivity measurements in Fig. 3(b). This is likely due to the new conformationally altered linear/expansion coil structure of the modified PEDOT: PSS. By using the modified PEDOT: PSS as the hole transport layer in the non-fullerene PBDBT: ITIC system, the power conversion efficiency of the organic solar cell was increased to 11.02%, compared to the control device with only PEDOT: PSS, which achieved an efficiency of 9.72%. Furthermore, the presence of the $Ti_3C_2T_x$ MXene nanosheet resulted in a power conversion efficiency of 14.55%, compared to the control device at 13.10% (Fig. 3d) with the active layer being a PM6:Y6 device. In addition, the performance stability of the device was boosted with the introduction of the $Ti_3C_2T_x$ MXene nanosheet, as shown in Fig. 3(e).

Researchers attempted to improve the performance of solar cells by adding titanium carbide nanosheets to zinc oxide to form a hybrid electron transport layer. This nanosheet improves the power conversion efficiencies of the cells by forming an "electron bridge" between the zinc oxide nanocrystals and coating them, which facilitates electron transfer and helps to passivate them. As a result, the cells based on the PBDB-T: ITIC, PM6:Y6, and PTB7:PC71BM photoactive layers saw improved power conversion efficiencies of 12.2%, 16.51%, and 9.36% respectively, compared to the control devices that only used the zinc oxide electron transport layers. Additionally, the systems that utilized the $Ti_3C_2T_x$/ZnO hybrid electron transport layers exhibited enhanced stability [50].

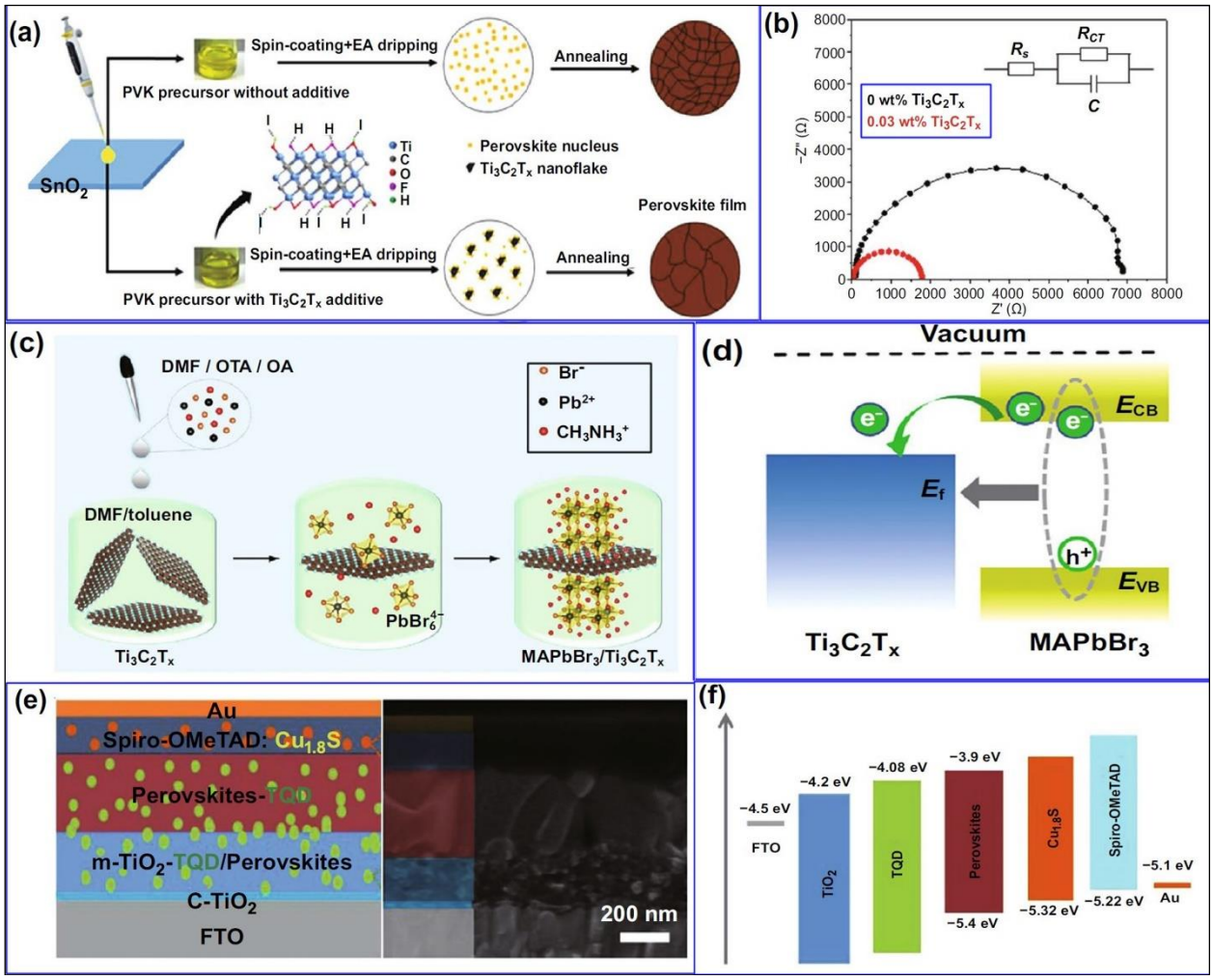

Fig. 2 - (a) The ways in which MAPbI3-based perovskite films arise and grow with or without the inclusion of titanium carbide ($Ti_3C_2T_x$); (b) a Nyquist plot was generated using a PV device at a bias of 0.7 Volts, with (or without) the addition of 3×10^(-2) weight percent of titanium carbide, in a dark environment; (c) a diagram showing the production of heterostructures made up of $MAPbBr_3$ and $Ti_3C_2T_x$, which is composed of multiple layers of titanium carbide nanosheets; (d) this graph illustrates that there is an electron transfer, with a corresponding energy level match between the $Ti_3C_2T_x$ nanosheet, which has a coating, and the $MAPbBr_3$ crystals; (e) a representation of the device's design is shown, as well as a cross-sectional SEM scan; (f) the depiction shows that the energy levels of the perovskite solar cell are in harmony with ultrathin titanium carbide ($Ti_3C_2T_x$) quantum dots, $Cu_{1.8}S$ in the Spiro-OMeTAD hole transport layer, and a combination of ETL/TiO_2 at the boundary [51]

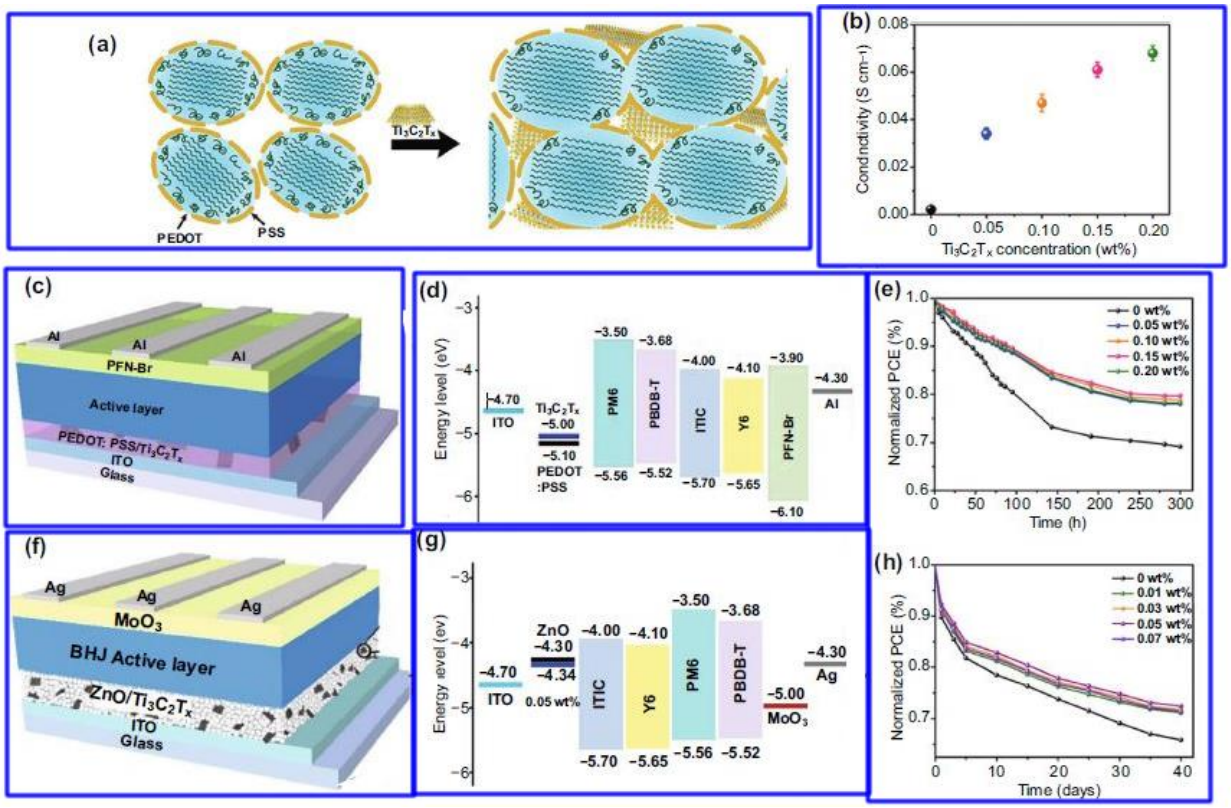

Fig. 3 - (a) Shows how modification took place in PEDOT: PSS concerning its structure and morphology. MXene ($Ti_3C_2T_x$) nanosheets were also incorporated into it; (b) on raw glass, the electrical conductivity of PEDOT: PSS was shown. This is with various additions of $Ti_3C_2T_x$; (c) configuration of the device; (d) an illustration of each organic solar cell component's energy level diagram. Here, $Ti_3C_2T_x$-modified PEDOT: PSS is used as the hole transport layer; (e) shows the test of stability for the different systems that have various addition of $Ti_3C_2T_x$. This addition took place in a nitrogen-regulated glove box, and it is based on the PBDB-T: ITIC as a light-absorbing layer; (f) configuration of the device; (g) the diagram shows the energy level of the different components of the organic solar cell. This was done by making use of $Ti_3C_2T_x$/ZnO as the electron transport layer; (h) shows the test of stability for the different devices as a result of PBDB-T: ITIC being a light-absorbing layer with the addition of $Ti_3C_2T_x$ in changing proportion. This addition is not an air-encapsulated one [51]

2.2 MXene as Electrode in Perovskite Materials

Recent research has found the electrical conductivity of the ($Ti_3C_2T_x$) MXene to be 15,100 Scm^{-1} [52]. This material also holds advantages such as high transparency, exceptional flexibility, and a tunable work function [7, 53, 54], making it a suitable electrode material for use in solar cells and other optoelectronic devices. Cao et al. (2019) demonstrated the effectiveness of this material in noble-metal-free $MAPbI_3$-based polymer solar cells by employing a straightforward hot-pressing technique [55].

In 2019, Fu et al. reported that $Ti_3C_2T_x$ solution was drop-casted on a grooved surface with an n^+-n-p^+ silicon solar cell to form an n^+ - silicon emitter (Fig. 4 a-c) [56, 57]. This setup led to an ohmic contact between the n^+ - Si and $Ti_3C_2T_x$, which was found to improve V_{oc} and J_{sc}, resulting in an increase in power conversion efficiency to 11.5 percent and a decrease in series resistance (Fig. 4f). Furthermore, rapid thermal annealing (RTA) was implemented for 30 seconds to enhance the physical adhesion and electrical contact between the n^+ - Si substrate and the MXene coating (Fig. 4d). The increasing slope of the J-V curves around V_{oc} (Fig. 4e) confirmed the result. Additionally, MXene can also be used in Schottky junction solar cells, as described by Yu et al. [58]. In these cases, MXene is formed with Si and serves as an electrode for charge collection as a transparent conducting film.

In 2019, Chen et al. reported a composite counter electrode (CE) for quantum dots sensitized solar cells (QDSCs) composed of copper mono-selenide nanoparticles (grown hydrothermally) on a sheet composed of $Ti_3C_2T_x$ nanosheets and graphite sheets screen-printed together [59]. This composite CE has higher electrical conductivity and a larger specific surface area than counter electrodes made of $Ti_3C_2T_x$ and CuSe. The larger surface area increases the number of active sites for polysulfide electrolyte reduction. Utilizing an ideal mass ratio, this $Ti_3C_2T_x$/CuSe composite CE resulted in QDSCs with a power conversion efficiency (PCE) of 5.12%, whereas devices with $Ti_3C_2T_x$ - and CuSe-based counter electrodes had PCEs of 2.04% and 3.47%, respectively. Tian et al. created a new composite CE composed of CuS/Ti_3C_2

through a simple ion exchange process at room temperature. This CE presented a higher electrocatalytic rate for polysulfide reduction when compared to the pure CuS [60]. As a result, the QDSC achieved an overall PCE of 5.11%, 1.5 times higher than the pure copper mono-selenide counter electrode. This was attributed to the combination of the catalytically active sites from the copper mono-selenide nanoparticles and the high conductivity of the titanium carbide (Ti_3C_2) skeleton. The next section of this article will go into greater detail about MXenes as HTLs/ETLs.

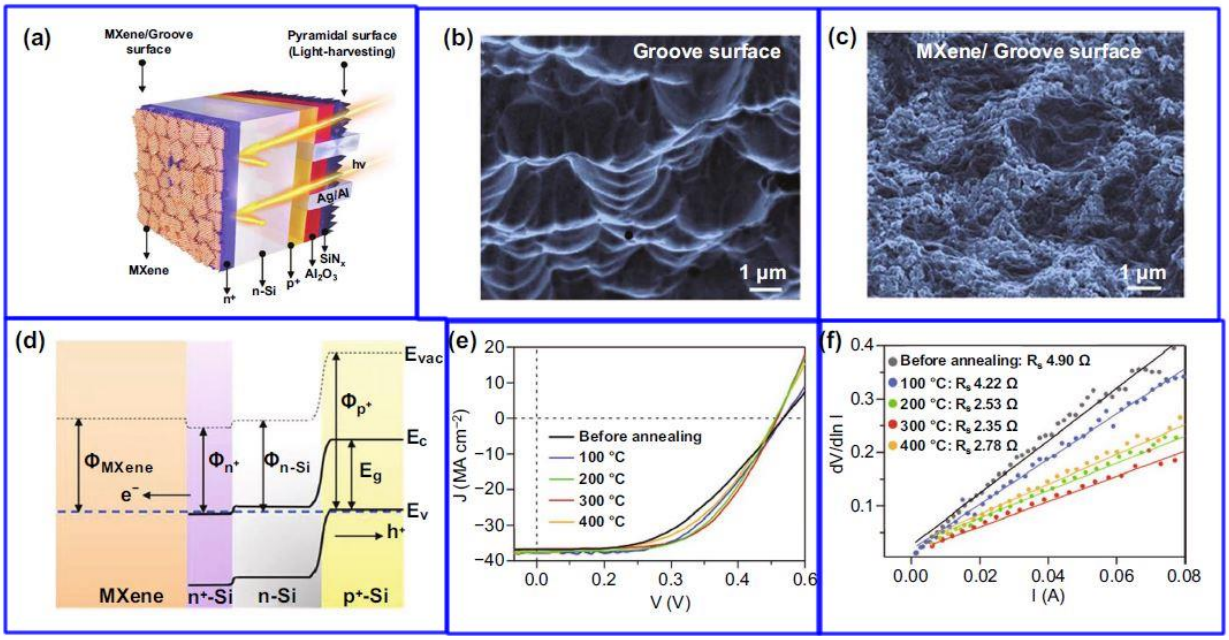

Fig. 4 (a) A diagram is presented that shows a silicon solar cell with an n^+ emitter and a $Ti_3C_2T_x$ electrode contact. This cell utilizes a combination of n^+–p–p^+ layers; (b) this demonstrates the SEM outcome of indentations on the n^+ side of the material before MXene coating; (c) the following demonstrates the result of scanning electron microscopy using an MXene coating; (d) Ev, Eg, and Ec are the valence band, energy bandgap, and conduction band of Si respectively; Φ is the energy level alignment, which is also known as the Work Function; (e) this graph displays the difference in the J-V curves before and after a 30-second thermal annealing treatment at varying temperatures; (f) the J-V measurement was used to calculate the series resistance of the samples before and after the rapid thermal annealing process [51]

2.3 Using Mxene as a Material for The Hole and Electron Transport Layers

Titanium carbide ($Ti_3C_2T_x$) has been found to have various work functions, which can be tuned when oxidized or reduced, according to a report by Yu et al. in 2019. They used UV-O_3/Hydrazine treatment to enhance the work function (ranging between 4.08 eV and 4.95 eV) of titanium carbide [61]. This has enabled $Ti_3C_2T_x$ to be employed as either a hole or electron transport layer in organic solar cells using a photoactive layer such as PBDB-T: ITIC, as illustrated in Fig. 5a. Devices that use $Ti_3C_2T_x$ as the hole transport layer have the ability to obtain a high PCE compared to other devices, with a PCE of 9.06% and 9.02% when used as an electron/hole-collection buffer layer, respectively (Fig. 5b). Additionally, it was discovered that V_{oc} rises throughout treatment, as seen in Fig. 5c. A report by Hou et al. in the same year also found that $Ti_3C_2T_x$ could be used as the hole transport layers in PBDB-T: ITIC-based organic solar cells to facilitate hole collection and transit, due to its exceptional metallic conductivity, energy-level alignment, and improved interface-contact, as shown in Fig. 5d [62]. Furthermore, when ITO was used as the hole transport layer, the PCE was 4.21% (Fig. 5e). This demonstrates the potential for $Ti_3C_2T_x$ to serve not only as additives and electrodes but also as a charge (hole/electron) transport layer in organic solar cells.

In 2019, Yu et al. reported the creation of a solar cell using an n-type Silicon and a titanium carbide ($Ti_3C_2T_x$) deposition. As illustrated in Fig. 6a, the $Ti_3C_2T_x$ served as the hole-collection electrode and the Schottky junction component with the n-type Si [58]. Additionally, oven transfer and floating procedures were used to deposit MXene onto some devices, producing J-V curves (illuminated) with initial efficiencies of 4.20% and 0.58%, as seen in Fig. 6b. Compared to the most advanced PEDOT: PSS-based device, the best titanium carbide-based device showed improved performance with a PCE comparison of 10.53 percent against 10.11 percent, as shown in Fig. 5f. Furthermore, the $Ti_3C_2T_x$ -based device had increased stability with no encapsulations when considering atmospheric conditions [63, 64].

The two-step chemical treatment of hydrochloric acid and gold (III) chloride can enhance the power conversion efficiency of oven-transfer devices to greater than 9%. With the addition of a polydimethylsiloxane (PDMS) antireflection

layer, a power conversion efficiency of more than 10% can be achieved. The key to suppressing carrier recombination appears to be the thin silicon oxide layer that forms between the $Ti_3C_2T_x$ and n-type silicon during oven transfer [65-68]. This layer can also be used to improve device performance. Both the conductivity of the MXene layer, due to the doping effect of hydrochloric acid, and the increased charge transfer from the gold nanoparticles formed by $AuCl_3$, are responsible for this improvement. An increase in the work function of the MXene layer from 4.80eV to 4.84eV and 4.93eV for the HCl, pristine and $AuCl_3$-treated samples, respectively, further contributes to the enhanced device performance [69].

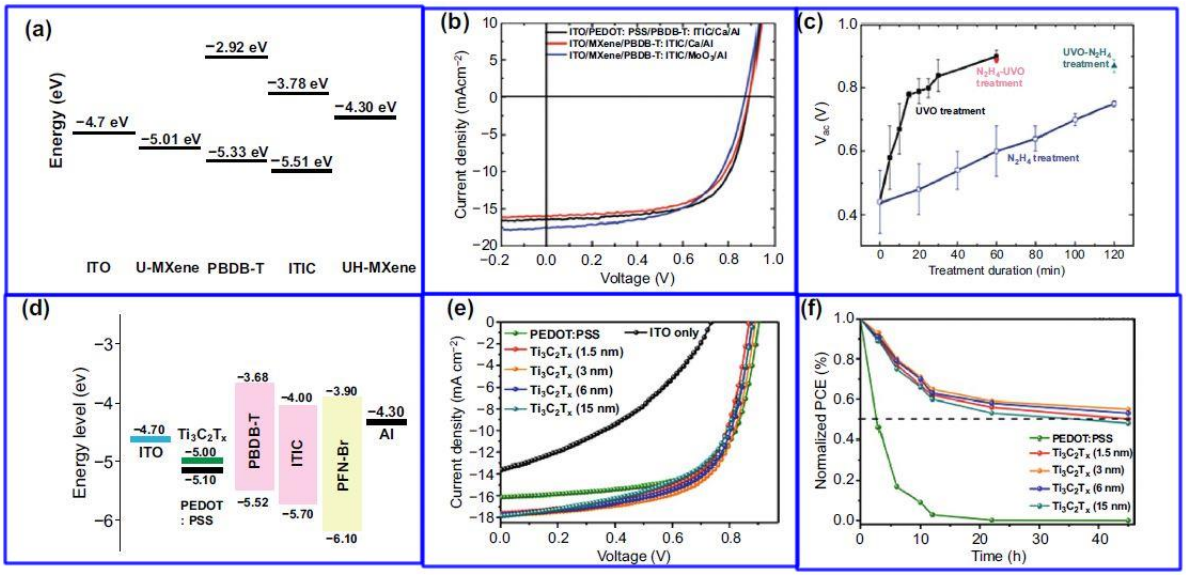

Fig. 5 - Titanium carbide treated with Hydrazine ($Ti_3C_2T_x$) is the high-temperature and electron transport layer when using UV-O_3 with PBDB-T and ITIC-based organic solar cells (a) different components possess different amounts of energy, measured in electron volts; (b) the J-V curves that are lit up represent the PBDB-T: ITIC-based Organic solar cells. U-MXene and UH-MXene refer to MXene that has been subjected to UV-O_3 and UV-O_3 followed by N_2H_4, respectively. U-MXene is utilized for capturing an electron in inverted OSCs, while UH-MXene is deployed for taking up a hole in typical OSCs; (c) the V_{oc} value of organic solar cells with titanium carbide ($Ti_3C_2T_x$) nanosheets as the hole transport layer is plotted on the y-axis against the duration of the treatment; (d) the positioning of the energy levels of the components; (e) plotting the voltage along the x-axis and the current density along the y-axis produces a distinct J–V curve that is illuminated; (f) the normalized PCE over time is used to measure the stability of atmospheric conditions without any protective coverings [51]

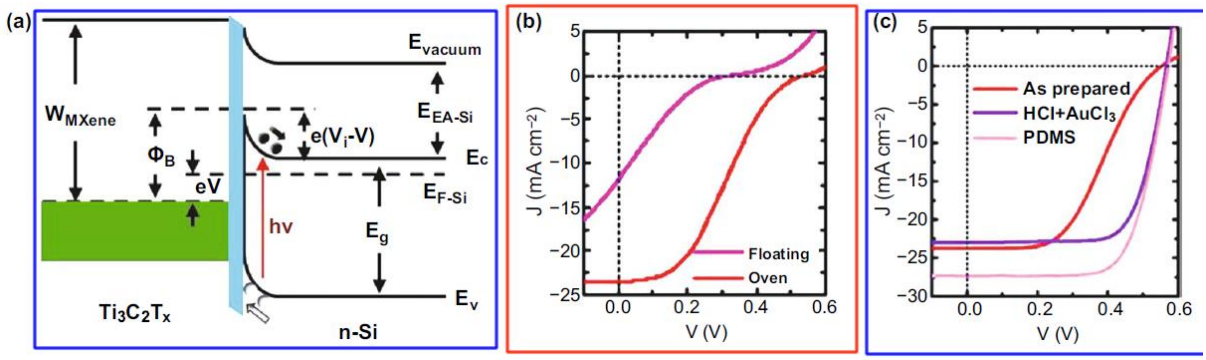

Fig. 6 - n-type Silicon solar cells coated with titanium carbide layers ($Ti_3C_2T_x$ MXene) (a) a presentation of the Energy-level of the major components with the light blue ribbon signifying the presence of a SiO_2 thin layer; (b) the diagram shows two curved lines which represent the J–V curves for the devices created by using both the oven and floating transfer techniques; (c) the J–V curves for devices made using the oven transfer method and then treated with a two-step chemical treatment (HCl + $AuCl_3$) are presented in an illuminated state, as well as after an antireflection coating of polydimethylsiloxane has been applied [51]

3. Conclusions

This review paper highlights the most recent advances in two-dimensional MXene research for solar cell applications. Specifically, quantum dot-sensitized solar cells and other types of solar cells (such as silicon wafer-based, perovskite, and organic solar cells) are the most typical solar cells where MXene can be applied as an electron, additive, and charge transport (i.e., hole or electron) layer. The majority of research concerning MXene has focused on $Ti_3C_2T_x$, the first MXene discovered at Drexel University in 2011. To better understand its potential applications in solar cells, this review begins by cataloging the various MXene syntheses. Despite being considered a promising material for high-performance or novel solar cell applications, MXene still faces challenges such as device performance (such as power conversion efficiency (PCE) and stability) that need to be addressed. Moreover, oxidation (exposure to air for an extended period) increases the material's resistance, thus lowering device performance. To make the most out of MXene's advantages, thorough theoretical and experimental approaches are necessary. It is believed that these intriguing MXenes will be able to contribute to clean energy conversion, flexible electronics, and the energy storage industry. To further advance MXene's applications in solar cells, the following four recommendations are proposed: (1) device performance (e.g. stability and PCE) should be improved by incorporating additional structures for light management and optimizing each interface in solar cells; (2) more research should be conducted (through experimental and theoretical simulations data) on the Fermi level and the different functional groups of MXenes, as this will provide more insight into the mechanisms of MXene; (3) MXene's properties, such as its high transparency, the abundance of electrochemically active sites, and adjustable electrical properties due to functional groups, should be taken advantage of to create more energy-serving devices, such as secondary batteries, PV supercapacitors, and advanced sensors; and (4) apart from $Ti_3C_2T_x$, other MXene-based solar cells should be explored (through unique combinations of properties while also tuning them by changing the ratios of M or X elements and also taking into account high performance-to-cost ratios).

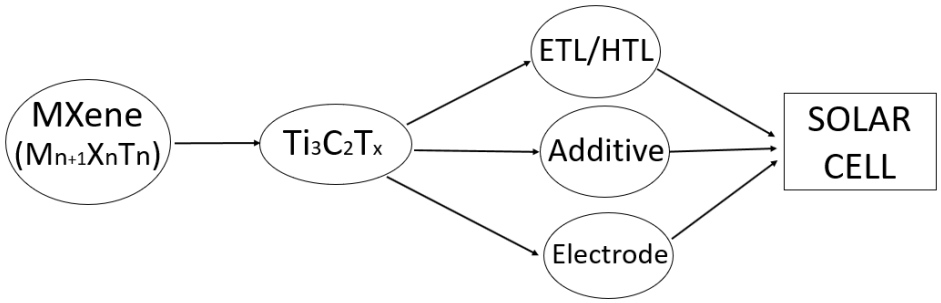

Fig. 7 - Summary of the application of MXene for photovoltaic application

Table 2 - Summary of characteristics of MXenes in solar cells

Role of MXenes	Summary of its application
Electron/Hole Transport Layer	One can easily adjust the carrier conducting characteristics and work functions.
Electrode	This material has adjustable work functions, high transparency, metallic conductivity, and remarkable flexibility.
	Various conducting nanomaterials, such as carbon nanotubes or metallic nanowires, are being used to create hybrid electrodes.
Additive	Similar to an "electron" bridge, there is an increase in the speed of electron movement.
	The conductivity and work function of the materials used for carrier transport is being adjusted.

Acknowledgement

The authors would like to thank the Department of Materials Science and Engineering, Hohai University, China, and the Department of Pure and Applied Physics, Ladoke Akintola University of Technology, Nigeria for their support.

References

[1] K. S. Novoselov *et al.,* "Electric field effect in atomically thin carbon films," *Science*, vol. 306, no. 5696, pp. 666–669, 2004.

[2] K. S. Novoselov *et al.,* "Two-dimensional atomic crystals," *Proc. Natl. Acad. Sci. U. S. A.*, vol. 102, no. 30, pp. 10451–10453, 2005.

[3] E. Bianco, S. Butler, S. Jiang, O. D. Restrepo, W. Windl, and J. E. Goldberger, "Stability and exfoliation of germanane: a germanium graphane analogue," *ACS Nano*, vol. 7, no. 5, pp. 4414–4421, 2013.
[4] B. Aufray *et al*., "Graphene-like silicon nanoribbons on Ag(110): A possible formation of silicene," *Appl. Phys. Lett*., vol. 96, no. 18, p. 183102, 2010.
[5] F.-F. Zhu *et al.*, "Epitaxial growth of two-dimensional stanene," *Nat. Mater*., vol. 14, no. 10, pp. 1020–1025, 2015.
[6] S. Shirvani, M. Ghashghaee, and K. J. Smith, "Two-dimensional nanomaterials in thermocatalytic reactions: Transition metal dichalcogenides, metal phosphorus Trichalcogenides and MXenes," *Catal. Rev. Sci. Eng*., pp. 1–51, 2021.
[7] K. Hantanasirisakul and Y. Gogotsi, "Electronic and optical properties of 2D transition metal carbides and nitrides (MXenes)," *Adv. Mater*., vol. 30, no. 52, p. e1804779, 2018.
[8] M. Naguib *et al.*, "Two-Dimensional Transition Metal Carbides," *ACS Nano*, vol. 6, no. 2, pp. 1322–1331, 2012.
[9] B. Anasori, M. R. Lukatskaya, and Y. Gogotsi, "2D metal carbides and nitrides (MXenes) for energy storage," *Nat. Rev. Mater*., vol. 2, no. 2, 2017.
[10] J.-C. Lei, X. Zhang, and Z. Zhou, "Recent advances in MXene: Preparation, properties, and applications," *Front. Phys*., vol. 10, no. 3, pp. 276–286, 2015.
[11] N. K. Chaudhari, H. Jin, B. Kim, D. San Baek, S. H. Joo, and K. Lee, "MXene: an emerging two-dimensional material for future energy conversion and storage applications," *Journal of Materials Chemistry A*, vol. 5, no. 47, pp. 24564–24579, 2017.
[12] I. M. Chirica, A. G. Mirea, Ş. Neaţu, M. Florea, M. W. Barsoum, and F. Neaţu, "Applications of MAX phases and MXenes as catalysts," *J. Mater. Chem. A Mater. Energy Sustain*., vol. 9, no. 35, pp. 19589–19612, 2021.
[13] M. Shekhirev, C. E. Shuck, A. Sarycheva, and Y. Gogotsi, "Characterization of MXenes at every step, from their precursors to single flakes and assembled films," *Prog. Mater. Sci*., vol. 120, no. 100757, p. 100757, 2021.
[14] J. Zhu *et al.*, "Recent advance in MXenes: A promising 2D material for catalysis, sensor and chemical adsorption," *Coord. Chem. Rev*., vol. 352, pp. 306–327, 2017.
[15] X. Zhan, C. Si, J. Zhou, and Z. Sun, "MXene and MXene-based composites: synthesis, properties, and environment-related applications," *Nanoscale Horizons*, vol. 5, no. 2, pp. 235–258, 2020.
[16] B. Ahmed, A. E. Ghazaly, and J. Rosen, "i -MXenes for Energy Storage and Catalysis," *Advanced Functional Materials*, vol. 30, no. 47, p. 2000894, May 2020
[17] F. Song, G. Li, Y. Zhu, Z. Wu, X. Xie, and N. Zhang, "Rising from the horizon: three-dimensional functional architectures assembled with MXene nanosheets," *Journal of Materials Chemistry* A, vol. 8, no. 36, pp. 18538–18559, 2020.
[18] C. Feng, Z. Wu, K. Huang, J. Ye, and H. Zhang, "Surface Modification of 2D Photocatalysts for Solar Energy Conversion," *Advanced Materials*, vol. 34, no. 23, p. 2200180, Apr. 2022.
[19] M. M. Hasan, M. M. Hossain, and H. K. Chowdhury, "Two-dimensional MXene-based flexible nanostructures for functional nanodevices: a review," *Journal of Materials Chemistry* A, vol. 9, no. 6, pp. 3231–3269, 2021.
[20] A. Agresti *et al.*, "Titanium-carbide MXenes for a work function and interface engineering in perovskite solar cells," *Nature Materials*, vol. 18, no. 11, pp. 1228–1234, 2019.
[21] P. O. Å. Persson and J. Rosen, "Current state of the art on tailoring the MXene composition, structure, and surface chemistry," *Curr. Opin. Solid State Mater. Sci*., vol. 23, no. 6, p. 100774, 2019
[22] X. Li, C. Wang, Y. Cao, and G. Wang, "Functional MXene Materials: Progress of Their Applications," *Chemistry - An Asian Journal*, vol. 13, no. 19, pp. 2742–2757, 2018.
[23] D. Xiong, Y. Shi, and H. Y. Yang, "Rational design of MXene-based films for energy storage: Progress, prospects," *Materials Today*, vol. 46, pp. 183–211, 2021.
[24] D. Johnson, Z. Qiao, E. Uwadiunor, and A. Djire, "Holdups in Nitride MXene's Development and Limitations in Advancing the Field of MXene," *Small*, vol. 18, no. 17, p. 2106129, 2022.
[25] Q. Tang, Z. Zhou, and P. Shen, "Are MXenes Promising Anode Materials for Li-Ion Batteries? Computational Studies on Electronic Properties and Li Storage Capability of Ti_3C_2 and $Ti_3C_2X_2$ (X = F, OH) Monolayer," *Journal of the American Chemical Society*, vol. 134, no. 40, pp. 16909–16916, 2012.
[26] F. Shahzad *et al.*, "Electromagnetic interference shielding with 2D transition metal carbides (MXenes)," *Science*, vol. 353, no. 6304, pp. 1137–1140, 2016.
[27] S. Kim *et al.*, "Enhanced adsorption performance for selected pharmaceutical compounds by sonicated $Ti_3C_2T_x$ MXene," *Chemical Engineering Journal*, vol. 406, p. 126789, 2021.
[28] X. Meng, X. Cui, N. P. Rajan, L. Yu, D. Deng, and X. Bao, "Direct Methane Conversion under Mild Condition by Thermo-, Electro-, or Photocatalysis," *Chem*, vol. 5, no. 9, pp. 2296–2325, Sep. 2019.
[29] N. H. Ahmad Junaidi, W. Y. Wong, K. S. Loh, S. Rahman, and W. R. W. Daud, "A comprehensive review of MXenes as catalyst supports for the oxygen reduction reaction in fuel cells," *International Journal of Energy Research*, vol. 45, no. 11, pp. 15760–15782, Jun. 2021.
[30] H. Wang *et al.*, "Clay-Inspired MXene-Based Electrochemical Devices and Photo-Electrocatalyst: State-of-the-Art Progresses and Challenges," *Advanced Materials*, vol. 30, no. 12, p. 1704561, Jan. 2018.

[31] Q. Zhong, Y. Li, and G. Zhang, "Two-dimensional MXene-based and MXene-derived photocatalysts: Recent developments and perspectives," *Chemical Engineering Journal*, vol. 409, p. 128099, Apr. 2021.
[32] H. Huang et al., "Noble-metal-free ultrathin MXene coupled with In2S3 nanoflakes for ultrafast photocatalytic reduction of hexavalent chromium," *Applied Catalysis B: Environmental*, vol. 284, p. 119754, May 2021.
[33] M. Malaki and R. S. Varma, "Mechanotribological Aspects of MXene-Reinforced Nanocomposites," *Advanced Materials*, vol. 32, no. 38, p. 2003154, Aug. 2020.
[34] A. Raza, U. Qumar, A. A. Rafi, and M. Ikram, "MXene-based nanocomposites for solar energy harvesting," *Sustainable Materials and Technologies*, vol. 33, p. e00462, 2022.
[35] C. Zhang et al., "Additive-free MXene inks and direct printing of micro-supercapacitors," *Nature Communications*, vol. 10, no. 1, Apr. 2019.
[36] Z. Zhang et al., "In Situ Growth of MAPbBr 3 Nanocrystals on Few-Layer MXene Nanosheets with Efficient Energy Transfer," *Small*, vol. 16, no. 17, p. 1905896, Mar. 2020.
[37] V. Natu, J. L. Hart, M. Sokol, H. Chiang, M. L. Taheri, and M. W. Barsoum, "Edge Capping of 2D-MXene Sheets with Polyanionic Salts to Mitigate Oxidation in Aqueous Colloidal Suspensions," *Angewandte Chemie International Edition*, vol. 58, no. 36, pp. 12655–12660, Aug. 2019.
[38] . J. Zhang *et al.*, "Oxidation Stability of Colloidal Two-Dimensional Titanium Carbides (MXenes)," *Chemistry of Materials*, vol. 29, no. 11, pp. 4848–4856, May 2017.
[39] Y. Chae *et al.*, "An investigation into the factors governing the oxidation of two-dimensional Ti_3C_2 MXene," *Nanoscale*, vol. 11, no. 17, pp. 8387–8393, 2019.
[40] T. S. Mathis *et al.*, "Modified MAX Phase Synthesis for Environmentally Stable and Highly Conductive Ti_3C_2 MXene," *ACS Nano*, vol. 15, no. 4, pp. 6420–6429, Apr. 2021.
[41] Z. Guo *et al.*, "High Electrical Conductivity 2D MXene Serves as Additive of Perovskite for Efficient Solar Cells," *Small*, vol. 14, no. 47, p. 1802738, 2018.
[42] Z. Wu *et al.*, "Enhanced performance of polymer solar cells by adding SnO_2 nanoparticles in the photoactive layer," *Organic Electronics*, vol. 73, pp. 7–12, Oct. 2019.
[43] Z. Wu *et al.*, "Bridging for Carriers by Embedding Metal Oxide Nanoparticles in the Photoactive Layer to Enhance Performance of Polymer Solar Cells," *IEEE Journal of Photovoltaics*, vol. 10, no. 5, pp. 1353–1358, Sep. 2020.
[44] Y. Wang *et al.*, "Enhanced performance and the related mechanisms of organic solar cells using Li-doped SnO_2 as the electron transport layer," *Materials Chemistry and Physics*, vol. 254, p. 123536, Nov. 2020.
[45] P. Shao *et al.*, "Facile embedding of SiO_2 nanoparticles in organic solar cells for performance improvement," *Organic Electronics*, vol. 50, pp. 77–81, Nov. 2017.
[46] A. Agresti et al., "Author Correction: Titanium-carbide MXenes for a work function and interface engineering in perovskite solar cells," *Nature Materials*, vol. 18, no. 11, pp. 1264–1264, Oct. 2019.
[47] V. Nicolosi, M. Chhowalla, M. G. Kanatzidis, M. S. Strano, and J. N. Coleman, "Liquid Exfoliation of Layered Materials," *Science*, vol. 340, no. 6139, Jun. 2013.
[48] X. Chen *et al.*, "Dual Interfacial Modification Engineering with 2D MXene Quantum Dots and Copper Sulphide Nanocrystals Enabled High-Performance Perovskite Solar Cells," *Advanced Functional Materials*, vol. 30, no. 30, p. 2003295, Jun. 2020.
[49] C. Hou and H. Yu, "Modifying the nanostructures of PEDOT: PSS/Ti3C2TX composite hole transport layers for highly efficient polymer solar cells," *Journal of Materials Chemistry C*, vol. 8, no. 12, pp. 4169–4180, 2020.
[50] C. Hou and H. Yu, "ZnO/ $Ti_3C_2T_x$ monolayer electron transport layers with enhanced conductivity for highly efficient inverted polymer solar cells," *Chemical Engineering Journal*, vol. 407, p. 127192, 2021.
[51] L. Yin, "MXenes for Solar Cells, '," *Nano-Micro Letters*, vol. 13, no. 1, pp. 1–17, 2021.
[52] J. Zhang *et al*., "Scalable manufacturing of free-standing, strong $Ti_3C_2T_x$ MXene films with outstanding conductivity," *Adv. Mater*., vol. 32, no. 23, p. e2001093, 2020.
[53] D. Xiong, X. Li, Z. Bai, and S. Lu, "Recent advances in layered $Ti_3C_2T_x$ MXene for electrochemical energy storage," *Small*, vol. 14, no. 17, p. 1703419, 2018.
[54] K. Li *et al*., "3D MXene architectures for efficient energy storage and conversion," *Adv. Funct. Mater*., vol. 30, no. 47, p. 2000842, 2020.
[55] J. Cao *et al.*, "Alternative electrodes for HTMs and noble-metal-free perovskite solar cells: 2D MXenes electrodes," *RSC Adv*., vol. 9, no. 59, pp. 34152–34157, 2019.
[56] H.-C. Fu *et al*., "MXene-contacted silicon solar cells with 11.5% efficiency," *Adv. Energy Mater.*, vol. 9, no. 22, p. 1900180, Apr. 2019.
[57] H. Fu *et al.*, "Solar Cells: MXene-Contacted Silicon Solar Cells with 11.5% Efficiency (Adv. Energy Mater. 22/2019)," *Advanced Energy Materials*, vol. 9, no. 22, p. 1970083, Jun. 2019.
[58] L. Yu, A. S. R. Bati, T. S. L. Grace, M. Batmunkh, and J. G. Shapter, "Ti $_3$ C 2 T x (MXene)-silicon heterojunction for efficient photovoltaic cells," *Adv. Energy Mater*., vol. 9, no. 31, p. 1901063, 2019.
[59] Y. Chen, D. Wang, Y. Lin, X. Zou, and T. Xie, "In suit growth of CuSe nanoparticles on MXene (Ti_3C_2) nanosheets as an efficient counter electrode for quantum dot-sensitized solar cells," *Electrochim. Acta*, vol. 316, pp. 248–256, 2019.

[60] Z. Tian, Z. Qi, Y. Yang, H. Yan, Q. Chen, and Q. Zhong, "Anchoring CuS nanoparticles on accordion-like Ti3C2 as high electrocatalytic activity counter electrodes for QDSSCs," *Inorg. Chem. Front*., vol. 7, no. 19, pp. 3727–3734, 2020.
[61] Z. Yu *et al*., "MXenes with tunable work functions and their application as electron- and hole-transport materials in non-fullerene organic solar cells," *J. Mater. Chem. A Mater. Energy Sustain*., vol. 7, no. 18, pp. 11160–11169, 2019.
[62] C. Hou, H. Yu, and C. Huang, "Solution-processable Ti3C2Tx nanosheets as an efficient hole transport layer for high-performance and stable polymer solar cells," *J. Mater. Chem. C Mater. Opt. Electron. Devices*, vol. 7, no. 37, pp. 11549–11558, 2019.
[63] L. Huang *et al.*, "Low-Temperature Growing Anatase TiO2/SnO2 Multi-dimensional Heterojunctions at MXene Conductive Network for High-Efficient Perovskite Solar Cells," *Nano-Micro Letters*, vol. 12, no. 1, Jan. 2020.
[64] Q. Zhou et al., "Tailored lattice 'tape' to confine tensile interface for 11.08%-efficiency all-inorganic CsPbBr3 perovskite solar cell with an ultrahigh voltage of 1.702 V," *Adv. Sci. (Weinh.)*, vol. 8, no. 19, p. e2101418, 2021.
[65] C. Xu, X. Zhao, M. Sun, J. Ma, and M. Wu, "Highly effective 2D layered carbides counter electrode for iodide redox couple regeneration in dye-sensitized solar cells," *Electrochim. Acta*, vol. 392, no. 138983, p. 138983, 2021.
[66] M. S. Ahmad *et al.,* "2-D Mxene flakes as a potential replacement for both TCO and Pt layers for Dye-Sensitized Solar cell," *Ceram. Int.*, vol. 47, no. 19, pp. 27942–27947, 2021.
[67] Y. Wang *et al.,* "MXene-modulated electrode/SnO_2 interface boosting charge transport in perovskite solar cells," *ACS Appl. Mater*. Interfaces, vol. 12, no. 48, pp. 53973–53983, 2020.
[68] L. Yang *et al.,* "Surface-modified metallic $Ti_3C_2T_x$ MXene as an electron transport layer for planar heterojunction perovskite solar cells," *Adv. Funct. Mater*., vol. 29, no. 46, p. 1905694, 2019.
[69] T. Chen *et al.,* "Accelerating hole extraction by inserting 2D Ti_3C_2-MXene interlayer to all-inorganic perovskite solar cells with long-term stability," *J. Mater. Chem. A Mater. Energy Sustain*., vol. 7, no. 36, pp. 20597–20603, 2019.